HHS Public Access

Author manuscript

Mol Cancer Ther. Author manuscript; available in PMC 2020 February 01.

Published in final edited form as:

Mol Cancer Ther. 2019 February ; 18(2): 267–277. doi:10.1158/1535-7163.MCT-18-0478.

Pleiotropic Action of Novel Bruton's Tyrosine Kinase Inhibitor BGB-3111 in Mantle Cell Lymphoma

Carrie J Li[#1], **Changying Jiang**[#1], **Yang Liu**[1], **Taylor Bell**[1], **Wencai Ma**[2], **Yin Ye**[3], **Shengjian Huang**[1], **Hui Guo**[1], **Hui Zhang**[1], **Lai Wang**[4], **Jing Wang**[2], **Krystle Nomie**[1], **Liang Zhang**[1], and **Michael Wang**[1,5]

[1]Department of Lymphoma and Myeloma, the University of Texas MD Anderson Cancer Center, Houston, Texas, USA

[2]Department of Bioinformatics and Computational Biology, the University of Texas MD Anderson Cancer Center, Houston, TX

[3]Department of Experimental Radiation Oncology, the University of Texas MD Anderson Cancer Center, Houston, TX

[4]BeiGene (Beijing) Co., Ltd., No.30 Science Park Road, Zhong-Guan-Cun Life Science Park, Changping District, Beijing P.R.China

[5]Department of Stem Cell Transplantation and Cellular Therapy, the University of Texas MD Anderson Cancer Center, Houston, TX

[#] These authors contributed equally to this work.

Abstract

Bruton's tyrosine kinase (BTK) is a key mediator of BCR-dependent cell growth signaling and a clinically effective therapeutic target in mantle cell lymphoma (MCL). The molecular impact of BTK inhibition remains unclear particularly in hematopoietic malignancies. We analyzed the molecular mechanisms of BTK inhibition with the novel inhibitor BGB-3111 (zanubrutinib) in MCL models. The efficacy of BGB-3111 was investigated using growth proliferation/cell viability and apoptosis assays in MCL cell lines and patient-derived xenograft (PDX) MCL cells. The activity and mechanisms of BGB-3111 were further confirmed using a cell line xenograft model, an MCL PDX mouse model, and a human phosphokinase profiler array and reverse phase protein array. Lastly, the mechanisms related to resistance to BTK inhibition were analyzed by creating cell lines with low levels of BTK using CRISPR/Cas 9 genome editing. We found that inhibition of BTK leads to suppression of tumor growth, which was mediated via potent suppression of Akt/mTOR, apoptosis, and metabolic stress. Moreover, targeted disruption of the BTK gene in MCL

Corresponding Author: Michael Wang, Department of Lymphoma and Myeloma, Unit 0429, The University of Texas MD Anderson Cancer Center, 1515 Holcombe Blvd., Houston TX, 77030, Phone: 713-792-2959; miwang@mdanderson.org.

Competing Financial Interests

Michael Wang, MD received a clinical trial grant to conduct a clinical trial with BGB-3111 in B cell lymphoma. The reagent BGB-3111 was provided by BeiGene Company free of charge. The laboratory research was not supported by BeiGene Company.

Disclosure of Potential Conflict of Interest

Michael Wang receives clinical research funding from BeiGene as well as Pharmacyclics, an AbbVie Company, and Acerta Pharma. All other authors declare no conflict of interest.

cells resulted in resistance to BTK inhibition and the emergence of novel survival mechanisms. Our studies suggest a general efficacy of BTK inhibition in MCL and potential drug resistance mechanism via alternative signaling pathways.

Introduction

Mantle cell lymphoma (MCL) is a subtype of non-Hodgkin's lymphoma characterized most frequently by cyclin D1 overexpression resulting from t (11;14)(q13;q32) chromosomal translocation (1–3).The incurable nature of MCL follows a familiar pattern of remission and relapse with progressively declining efficacy and increasing frequency of resistance, and treatment alternatives are urgently needed (1–3).

An unusual degree of complexity found in MCL tumors has impeded the research efforts to identify characteristic mutations and predictive/prognostic markers (4). At a minimum, MCL pathogenesis involves cell cycle and transcriptional deregulation, aberrant expression of apoptosis regulators, and impaired DNA damage response pathways (4,5). Recently, high throughput screening has identified the importance of B-Cell Receptor (BCR)-driven NF-κB signaling, similar to that of ABC-DLBCL, in determining response to therapies targeting NF-kB (6,7).

FDA approval of ibrutinib in 2013 was a milestone for MCL therapy; however, many details regarding how ibrutinib and its target Bruton's tyrosine kinase (BTK) regulate downstream survival pathways and other signaling cascades remain unclear as of today. Clinical demonstrations of BTK as an actionable target in various B-cell malignancies have prompted concurrent development of more selective BTK inhibitors and BTK-focused research efforts (8–11).

The emergence of ibrutinib-resistant disease and subsequent studies have uncovered potential contributors to ibrutinib resistance in MCL, including acquired BTK mutations that interfere with ibrutinib binding or aberrant upregulation of PI3K (12,13). Assessment of novel BTK inhibitors therefore provides a valuable platform to study BTK as a rational therapeutic target and to probe the role of BTK in ibrutinib resistance.

BGB-3111(zanubrutinib) (14) is a novel and selective BTK inhibitor that has been reported to possess greater specificity for BTK and has a smaller proportion of off-target effects compared with ibrutinib. Preliminary clinical data of BGB-3111 in B-cell malignancies indicate that BGB-3111 exhibits excellent efficacy in MCL (11,15). In this report, we assessed the *in vitro* and *in vivo* efficacy of BGB-3111 in preclinical MCL models and identified potential mechanisms mediating therapeutic resistance.

Materials and Methods

Reagents & Cell Culture

BGB-3111 was provided by BeiGene (Beijing, PR China). Human MCL cell lines (Jeko-1, Z-138, Mino, Maver-1, Rec-1, JVM-2, & JVM-13) were maintained in RPMI 1640 supplemented with 1% Penicillin/streptomycin, 25 mM 4-(2-hydroxyethyl)-1-

piperazineethanesulfonic acid (HEPES), 10% FBS (Sigma, St. Louis, MO, USA) and 1× Glutamax (Sigma). Cells were cultured in 37°C tissue culture CO_2 incubator. Cell lines were authenticated by single-nucleotide polymorphism profiling fingerprinting.

Cell Viability Assay

Cells were seeded at 10,000 cells per well (MCL cell lines) or 125,000 cells per well (primary cells) in 96-well plates and treated with various doses of compounds in triplicate. Cell viability was measured following 72 hr (cell lines) or 24 hr (primary cells) incubation. Cells were lysed with CellTiter-Glo Luminescent Cell Viability Assay Reagent (Promega, Madison, WI, USA), and luminescence was quantified using BioTek synergy HTX Multi-mode microplate reader. Each triplicate experiment was performed no less than three times to construct the cell survival curve.

Immunoblotting

Whole cell lysates were obtained using the Complete Mini Protease Inhibitor Cocktail (Roche, Indianapolis, IN, USA) in RIPA buffer (Bio-Rad, Hercules, CA, USA) and quantitated with the Quick Start™ Bradford Protein Assay Kit (Bio-Rad). Protein samples were electrophoresed on (Bio-Rad) and transferred to PVDF membranes. Primary antibodies to detect total and phosphorylated proteins, and their sources are listed in Supplementary Materials and Methods.

Annexin V/PI Apoptosis Assay

Flow cytometry for the measurement of apoptosis was performed with a BD LSRFortessa™ (BD Biosciences, Oxford, UK). BGB-treated cells were fixed and stained with Annexin V and propidium iodide (PI) (Abcam, Cambridge, UK).

Phospho-kinase Profiler Array

The human phospho-kinase profiler array (R&D Systems, Minneapolis, MN) was utilized according to the manufacturer's protocol. Positive signals developed on X-ray film were analyzed using ImageJ (Wayne Rasband, National Institutes of Health (NIH), Bethesda, MD, USA).

Reverse-Phase Protein Array (RPPA) and Data Statistical Analyses

RPPA data was produced by MD Anderson RPPA Core Facility. A total of 30 samples from 2 cell lines (Jeko-1 & Mino), 3 time points (0, 6, 24 hr), and 3 treatments (10 μM BGB-3111, control) were subjected to RPPA analysis. For each condition, there were 3 biological replicates. The slide image was quantified by using MicroVigene 4.0 (Vigene-Tech, Carlisle, MA). The spot level raw data were processed by using the R package Super Curve, developed in house (https://r-forge.rproject.org/projects/supercurve), which returns the estimated protein concentration (raw concentration) and a quality control (QC) score. The raw concentration data were normalized by median-centering each sample across all the proteins to correct loading bias.

One-way ANOVA was used to compare the 24 hr, 6 hr and 0 hr samples in the same cell line and same drug treatment. A Beta-Uniform Model (BUM) was applied to the resulting p-

values in order to adjust for multiple hypothesis testing and to estimate False Discovery Rate (FDR). In each comparison, $p \leq 0.05$ (corresponding FDR ranges from 0.03 to 0.06) with $|\text{average fold change}| \geq 1.23$ threshold were used to select the differentially expressed proteins. A two-way hierarchical clustering heatmap was drawn using significant proteins from the ANOVA analyses. Pearson distance metric and Ward's minimum variance method was used for samples and genes clustering in the heatmap. Data statistical analyses were performed using R, a publicly available statistical computing tool (https://www.r-project.org/).

CRISPR-Cas9-mediated Gene Editing

BTK knockdown cell lines were generated using the CRISPR/Cas9 genome editing system. BTK-specific guide RNA (gRNA) expression vectors were generated as described (16,17). Two CRISPR guide sequences targeting BTK are: gRNA1 targeting BTK Exon 2: GATGCTCTCCAGAATCACTG, and gRNA2 targeting BTK Exon 18: TGTGGGAAATTTACTCCCTG. Following transfection and single cell seeding in 96-well plates, western blots were used to screen for BTK-null clones as the primary approach. Candidate clones negative for BTK expression were subjected to genotyping to identify indels from both alleles. Ten or more clones of each genomic PCR fragment were sequenced to confirm the knockdown genotype (Fig. S1). The genetic identities of BTK-KD cell lines were validated by Sequenom Pro SNP fingerprinting in which all 44 marker sites matched completely.

Generation of the Stable Luciferase Reporter

Pseudo-viruses carrying the dual reporters GFP and Luciferase under the promoter of CMV or NF-κB were produced in HEK293FT cells *via* cotransfection of pGreenFire1-CMV or pGreenFire1-NF-κB respectively, with its packaging plasmids pCMV-VSV.G and pCMV-d82 and used to infect Jeko cells. The infected cells were subsequently sorted for GFP-positive cell population at 4 days post-infection. After expansion for 1 week, the stable luciferase reporter cells were validated by flow cytometry to check for GFP expression and by luciferase assay to check for luciferase expression and activity. The resulting stable cells were named Jeko-CMV-Luc and Jeko-NF-κB-Luc.

Luciferase Assay

Jeko-CMV-Luc and Jeko-NF-κB-Luc cells were treated with BGB at 0, 5, 15 μM, for 12 and 24 hours. The cells were harvested and subjected to luciferase assay to measure luciferase activity using firefly luciferase assay system (Promega) according to manufacturer's protocol. The luciferase activity in Jeko-NF-κB-Luc cells was first normalized to that in Jeko-CMV-Luc cells for the same treatment condition. The luciferase activity in treated samples of Jeko-NF-κB-Luc cells were further normalized to that in the untreated control. Fold of NF-κB activity are presented. The experiment were performed in independent triplicate.

BGB-3111 in patient-derived xenograft (PDX) MCL Model

MCL PDX mice were generated according to previously described methods (18). All experimental procedures and protocols were approved by the 'Institutional Animal Care' and 'Use Committee of The University of Texas MD Anderson Cancer Center'. In total, 25 NSG (Nod SCID Gamma) mice (The Jackson Laboratory, Bar Harbor, Maine, USA) were inoculated and 15 of which with eligible MCL tumor size and comparable β_2M levels were randomized into three treatment groups: 1) vehicle control (n=5) and 2) 30 mg/kg BGB-3111 oral gavage BID (n=5). Powdered drug was prepared in a methycellulose suspension immediately preceding administration. Mice were monitored for tumor growth, and initial tumor burden preceding treatment was determined by tumor volume measurements and detection of circulating human β_2M levels by ELISA (Abnova, Taipei, Taiwan). Mice were treated and monitored for 25 days; and sacrificed due to morbidity issue in the control group. Following animal sacrifice/death, tumor tissue and mouse spleens were excised and fixed in formalin for histopathological staining.

Rec-1 MCL xenograft model

Rec-1 tumor cells were implanted subcutaneously in female NOD/SCID mice. On day 3 after inoculation, the mice were randomly divided into six groups (n=10) and treated for 20 days as indicated. Tumor volume was measured twice weekly.

Animal study approval

All experimental procedures and protocols were approved by the 'Institutional Animal Care' and' Use Committee of The University of Texas MD Anderson Cancer Center.'

Results

BGB-3111 inhibits MCL cell proliferation and induces apoptosis

BGB-3111 belongs to a class of covalent ATP-competitive inhibitors designed to inhibit the BTK catalytic domain. As BTK is highly active in MCL and promotes MCL survival and growth, we determined the ability of BGB-3111 to inhibit MCL cell proliferation. Cell growth inhibition as measured by cell density was readily detectable following 72 hr incubation at 5 μM and 15 μM (Fig. 1A). Cell survival was also measured in six MCL cell lines treated with escalating doses of BGB-3111 for 72 hr (Fig. 1B). The IC_{50} values were 1.487 μM and 5.884 μM in the known BTK inhibitor-sensitive lines, Jeko and Mino, respectively, and the highest IC_{50} value of 81.55 μM observed in the JVM-13 MCL cell line. These results suggest that BGB-3111 is strongly cytostatic towards MCL cells in cultured conditions with a dose range and individual MCL cell line response similar to ibrutinib. BTK auto-phosphorylation is a direct indicator of its functional activation; therefore, we confirmed the ability of BGB-3111 to suppress phospho-BTK. BGB-3111 potently inhibited BTK phosphorylation in Jeko-1 and Mino MCL cell lines at nanomolar concentrations (Fig. S2A). The concentration that inhibits the phosphorylation is vastly lower than the concentration needed to observe cellular effects, which is common for kinase inhibitors. Furthermore, 5 μM BGB-3111 was sufficient to suppress BTK activation extending to 48 hr (Fig. S2B).

To dissect the cellular basis of BGB-3111-mediated anti-proliferative activity, we tested whether BGB-3111 treatment leads to apoptosis. Mino and Maver-1 MCL cell lines exhibited dose-dependent increases in apoptosis at doses below BGB-3111 IC_{50}, suggesting that apoptosis may partially underlie the observed decrease in cell proliferation (Fig. 2A). When primary MCL cells isolated from PDX mouse tumor tissue were tested, strong induction of apoptosis was observed at much lower BGB-3111 doses (1 and 3 μM) compared with immortalized MCL cells (Fig. 2B).

The onset of apoptosis by BGB-3111 was further corroborated by apoptotic molecular markers (Fig. 2C). Jeko-1, Mino, and Rec-1 cells exposed to BGB-3111 demonstrated significant dose-dependent increases in PARP and caspase-3 cleavage. Similarly, PDX tumor cells treated with BGB-3111 exhibited appreciable increases in PARP cleavage compared with untreated cells (Fig. 2D). We subsequently determined the temporal effects of BGB-3111-induced apoptosis by analyzing four MCL cell lines treated with BGB-3111 for 0, 24, and 48 hr (Fig. 2E). In Jeko-1 and Maver-1, prolonged exposure to BGB-3111 yielded a substantial increase in apoptosis, suggesting a diverse temporal response between MCL cell lines for cell death.

Antitumor efficacy of single agent BGB-3111 in subcutaneous mouse models

Given the anti-proliferative effects of BGB-3111 in cellular models, we determined its antitumor activity in cell line and PDX mouse models. In a Rec-1 xenograft model (Fig. 3A), BGB-3111 strongly inhibited tumor growth at 2.5 mg/kg BID and 7.5 mg/kg BID, with saturation of observable benefit at 24.9 mg/kg BID.

Next, we examined tumor growth inhibition by BGB-3111 in an MCL PDX model derived from a treatment-naïve patient who responded to ibrutinib. To determine the appropriate BGB-3111 dose to apply in the MCL PDX mouse model, a pilot study was performed and showed that twice-daily administration (BID) of BGB-3111 appeared more effective than the equivalent dose administered once-daily (QD) (Fig. S3). Given the aggressiveness of the MCL PDX model, 30 mg/kg BID was used to treat the mice. BGB-3111-treated mice presented no detectable toxicities, and maintained overall weight in comparison to control mice. Mice treated with BGB-3111 30 mg/kg BID demonstrated significantly deterred tumor growth compared to vehicle mice (Fig. 3B). We further validated tumor burden between BGB-3111 and vehicle groups by measuring tumor weight following sacrifice (Fig. 3C). At day 25, the mean tumor volumes were 1.607±255 mm^3 for the vehicle group and 504±352 mm^3 for the BGB-3111 group. Consistent with findings of tumor growth inhibition by volume, mean tumor weights resected from BGB-311 mice weighed significantly less than those of the vehicle-treated cohort (Fig. S4). Moreover, post-treatment sacrifice also revealed that mice treated with BGB-3111 presented insignificant spleen enlargement compared with the vehicle-treated group (Fig. 3C).

BTK inhibition by BGB-3111 disrupts Akt/mTOR signaling and NF-κB function

The potent antitumor activity of BGB-3111 in MCL *in vivo* models led us to investigate the underlying mechanisms of BTK inhibition. To identify the prevalent molecular effects of BTK inhibition, we analyzed the phosphorylation status of 43 cytoplasmic kinases in

BGB-3111-treated MCL cells using a phosphokinase array (Fig. 4A-B). In both Jeko-1 and Mino cells, BTK inhibition by BGB-3111 resulted in significant suppression of Akt and GSK3 α/β activation, suggesting that compromised function of these two proteins are important effectors of BTK inhibition.

The ability of BGB-3111 to acutely affect growth and survival signaling pathways was further verified in Jeko-1, Maver-1, and Z-138 cells (Fig. 4C) with 5 μM treatment to minimize the off-target and secondary effects. BGB-3111 treatment resulted in rapid Akt (Ser473) phosphorylation attenuation, with significant reduction observed after treatment in Jeko-1 and Maver-1 cells. However, recovery of phospho-Akt was observed at 1 hr and 3 hr after treatment in Z138 cells. The Akt/mTOR substrate p70S6K displayed a similar recovery at 3 hr. after an initial phosphorylation loss in Jeko-1 and Z138 cells. These results suggest an adaptive rebound of Akt /mTOR signaling from MCL cells treated with low doses of BGB-3111. To examine the sustained suppression of the signaling pathways under therapeutically relevant conditions, we exposed Jeko-1 and Mino cells to The BGB-3111 IC_{50} dose of 15 μM and analyzed the impact on Akt and BTK pathways at 6, 12, and 24 hr (Fig. 4D). While phospho-BTK remained fully suppressed at all the time points treated with BGB-311, phospho-Akt recovered in both cell lines at 12 hr after exposure, again suggesting an adaptive rebound of Akt signaling by MCL cells. However, p-P70S6K and p-PLCγ2 exhibited sustained decrease in Jeko-1 cells, indicating the recovery of phospho-Akt alone is not sufficient to revert the inactivation of proliferation and survival factors in MCL cells upon BTK inhibition.

To further define the drug response profile of BGB-3111, we performed RPPA analysis on Jeko-1 and Mino cells treated with BGB-3111 (Fig. 5A-B). In both Jeko-1 and Mino cells, inhibiting BTK resulted in the suppression of Akt/mTOR signaling, including potent suppression of p70S6K and S6 activation (19–21) (Fig. 5C). In Mino cells, BTK inhibition also induced inactivation of the catalytic p110 PI3K subunit, suggesting that BTK inhibition in MCL acts primarily along the PI3K/Akt/mTOR axis.

BTK inhibition induced caspase 3 and 7 cleavage and modulation of BCL-2 family proteins, suggesting that the potent antitumor activities of BGB-3111 may act through suppression of AKT/mTOR signaling and induction of cell death via cell apoptosis. To validate these findings, the differential protein expression was verified in Jeko-1 and Mino cells upon treatment with BGB-3111 at the same experimental conditions as in the RPPA analysis. Consistently, we found that BTK activation was suppressed constantly upon BGB-3111 treatment (Fig. 5C). Rather, the AKT/P70-S6K/S6-axis showed a dynamic inhibition pattern upon BGB-3111 treatment, which, however again, was not sufficient to overcome the BTK inhibition-induced cell apoptosis, evident by caspase 3 cleavage (Fig. 5C). RPPA analysis also revealed additional down regulation of metabolic enzymes such as FASN and ACC1, suggesting that BTK inhibition by BGB-3111 is accompanied by restricting cellular metabolism. These results provide the mechanistic basis of the apoptotic response in MCL cells upon BTK inhibition. However, when we examine the BCL-2 family proteins, we failed to identify the pro-apoptotic or anti-apoptotic protein(s) that are responsible for BGB-3111-induced cell death (Fig. 5C), which suggests that additional pathways contribute to BGB-3111-induced cell death. It is well known that constitutive NF-kB activation is the

hallmark of MCL; therefore, we examined whether BGB-311 treatment suppresses NF-kB activation. Given that p-p65 may not be an obligate marker for NF-κB activity, we performed a functional assay to determine the effects of BGB-3111 treatment on the NF-kB pathway. We measured NF-κB activity in Jeko cells with a reporter construct in which expression of a bicistronic GFP/luciferase cassette is driven by tandem repeat of five NF-kB response elements and detected marked reductions (≈ 50%) of NF-kB-mediated transcription activation at 12 and 24 hr after BGB-3111 treatment (Fig. 5D), suggesting that BTK inhibition effectively suppresses NF-κB activity.

Loss of BTK confers resistance to BTK inhibitors

In both frontal and acquired ibrutinib resistance, MCL cells are able to circumvent BTK inhibition, suggesting the activation of alternative growth signaling pathways in resistant cells; therefore, we targeted the BTK locus in Jeko cells to obtain a loss-of-function BTK cellular model.

We generated two independent protein hypomorph mutants, BTK-KD1 and BTK-KD2, via CRISPR/Cas9-mediated gene editing (Fig. 6A, Fig. S1) (16). We believe that the BTK levels are minimal because the intact allele may reside on the inactivated X chromosome as the Jeko cells were derived from a female MCL patient; therefore, leaky expression of BTK may occur, producing low levels of BTK. Despite the marked decrease of BTK protein, these mutant cells proliferated normally, indicating that compensatory growth signaling may be activated in the absence of BTK. To confirm this notion, we tested whether the BTK KD cells remain sensitive to BTK inhibition and found that both mutants are profoundly refractory to BGB-3111 (Fig. 6B), as reflected by a 5- to10-fold increase in their IC_{50} values. More importantly, these experiments revealed the ability of Jeko, and perhaps MCL cells in general, to circumvent the unavailability of BTK-dependent signaling by activating and adapting to alternative pro-proliferation mechanism(s). To identify potential pathways giving rise to resistance to BTK inhibition, we performed phosphokinase array analysis to determine whether the drug-resistant manipulated BTK cells exhibited steady-state signaling profiles different from the isogenic parental cell Jeko-1. The comparative study revealed two significantly elevated factors, P70S6K and WNK1, different between the BTK KD cells and drug-sensitive parental cells (Fig. 6C). P70S6K is a hallmark of the mTOR pathway activation and constitutively activated in MCL. Wnk1 kinase, on the other hand, has not been previously described in the context of MCL. These results suggest that drug-resistant MCL cells possess BTK-independent survival mechanisms, at least in part through the activation of mTOR.

To address this further, RPPA analysis was performed and showed that the BTK KD1 and BTK KD2 cells are clearly distinct from their parental Jeko-1 cells (Fig. 6D), predominantly through three pathways that are essential for cell survival and cell proliferation: enhanced AKT/mTOR signaling and NF-kB signaling and a diminished DNA repair response. These findings were further verified by immunoblotting (Fig. 6E) in Jeko, BTK KD mutants and Jeko R cells, which became ibrutinib- and BGB-3111-resistant after chronic exposure to ibrutinib (Fig. S5A). Thus, MCL cell growth in the absence of normal BTK function likely requires the activation of all of these survival pathways. Indeed, we found that constitutive

activation of both pathways in drug-resistant BTK KD mutants and Jeko R cells, which became ibrutinib- and BGB-3111-resistant after chronic exposure to ibrutinib, but not the drug-sensitive parental cells (Fig. 6E) reflected by the substantial increases in phosphorylation of PLCγ2, AKT, and S6. These results suggest that the stable augmentation of the AKT and NF-kB pathways is the mechanistic basis of evading BTK inhibition.

To substantiate the effects of constitutively active survival pathways, we analyzed p-PLCγ2, p-AKT, p-P70S6K, p-S6 in BTK KD cells. As shown (Fig. 6F), the phosphorylation of p-P70S6K and p-S6 exhibited resistance to BTK inhibition by BGB-3111 in the BTK mutant (IC_{50} = 16.2 μM) and Jeko R (IC_{50} = 17.8 μM) cells, but not in the BTK-proficient parental Jeko cells (IC_{50} = 1.5 μM) or other MCL cell lines with either sensitivity or resistance to BGB-3111 such as Mino (IC_{50} = 5.9 μM) and Maver (IC_{50} = 5.9 μM), suggesting that constitutively active survival pathways indeed lead to the augmented survival signaling. Additionally, both total and phospho-Wnk1 are drastically increased in the BTK KD and Jeko R cells compared to the parental cells, confirming the phosphoprotein array results (Fig. 6F). We also confirmed whether NF-kB activation is altered upon BGB-3111 treatment in BTK KD cells. In contrast to that of parental Jeko-1 cells, BGB treatment had an insignificant effect in inhibiting NF-kB signaling in the functional NF-kB reporter assay (Fig. 5D). Altogether, the elevated survival signaling activation in BGB-3111 resistant cells underlies the resistance to BTK inhibition, cell survival, and growth in a BTK-independent manner.

Discussion

BTK modulates key proliferation and survival pathways in B cells, and targeting BTK has achieved remarkable clinical efficacy in MCL. In this work, we obtained strong evidence that BGB-3111 is a potent inhibitor of BTK and demonstrated its single agent preclinical efficacy. We show that BTK inhibition in MCL cells causes pleiotropic effects, which is likely an important prerequisite for the anti-proliferative impact. Conversely, we found that constitutive activation of multiple growth and survival signaling mechanisms appear to be involved in acquired resistance to BTK inhibition.

Using both RPPA and phosphokinase profiling, we found that BGB-3111 treatment resulted in pleiotropic effects on multiple MCL survival mechanisms. The affected pathways in different MCL cells included suppression of PKCβII, a key transducer of NF-κB and MAPK/ERK, inhibition of AKT and AKT-substrates glycogen synthase kinase (GSK) and mTOR, down regulation of Ras family kinases, and activation of the executioner caspase-7. A decrease in ATM levels was also observed in Jeko cells subjected to BTK inhibition and in BTK KDs (Fig. S5B-C) as well as in Mino cells treated with BGB-3111 (Fig. 5, Fig. S5D). Furthermore, a number of factors downstream of ATM was also examined and P21 and p-AMPK were downregulated upon BGB-3111 treatment. Interestingly, p53 remained unchanged in the Mino cell line and was undetectable in the Jeko cell line, which is known to be mutant for p53 (Fig. S5D). Overall, weakened ATM function may render MCL cells more prone to endogenous damage, contributing to growth inhibition.

Previous studies investigating alternate therapeutic targets have suggested that MCL-1 downregulation sensitizes MCL to BCL-2 inhibition, and the combinatorial efficacy of ibrutinib and the BCL-2 inhibitor ABT-199 has clearly been demonstrated (22–24). Our proteomic profiling identified the downregulation of MCL-1 by BGB-3111 in Jeko cells. Thus, further exploration regarding the identification of novel targets in the drug resistance mutants should be beneficial. Given that BTK inhibition severely hampers MCL proliferation, it was unexpected that a BTK mutant with exceedingly low levels of BTK would be viable. Our finding that MCL cells are able to adapt to BTK-independent survival can potentially explain the majority of drug resistance cases and could elucidate mechanisms of metastasis Treatment in a PDX MCL model also revealed an additional benefit in prevention of spleen metastases with BGB-3111 (Fig. 3C). Indeed, BGB-3111 potently inhibited cell adhesion of drug-sensitive Jeko cells, but not drug-resistant BTK KD2 cells, to stromal cells (Fig. S6).

We found that drug-resistant BTK KD cells are accompanied by constitutive activation of key BCR downstream targets Akt, and p65. Interestingly, BTK inhibition of BTK KD cells repressed constitutive Akt and p-p65 activation similarly to the effects observed in normal MCL cell lines.

Phospho-proteomic profiling of BTK-KD mutants uncovered dramatic p70S6K and Wnk1 increases compared with the parental BTK-proficient Jeko-1 cells. While p70S6K upregulation likely counteracts suppression of mTOR signaling induced by BTK inhibition, Wnk1 upregulation is intriguing. Wnk1 belongs to the family of unusual serine/threonine Wnk (with no lysine [K]) protein kinases that serves as a broad range of cell-specific functions, including regulation of ion homeostasis and neuron depolarization (25–28). Kochl *et al* reported a regulatory role for Wnk1 in T-lymphocyte migration and adhesion (29), and RNA interference screening previously identified Wnk1 as an Akt substrate with potential functionality as a negative regulator of cell proliferation in adipocytes (30). Activation of this protein in MCL implicates a heretofore undefined role for Wnk1 in BCR signaling.

Targeted therapy against BTK has yielded unprecedented clinical benefit for MCL patients and is being explored in other major hematopoietic malignancies (8). BGB-3111 as a novel BTK inhibitor offers a new option for targeting BTK, and our findings provide mechanistic dissection of signaling response to this important treatment strategy. The BTK genetic model revealed a potential drug resistance mechanism and, more importantly, established a platform to detect and identify therapeutic targets to counter resistance.

Supplementary Material

Refer to Web version on PubMed Central for supplementary material.

Acknowledgments

This study was supported by the NIH-funded Cancer Center Support Grant (CCSG) P30 CA016672 and the R21 CA202104 (Michael Wang, PI). This study was also partially supported by the generous philanthropic support to the MD Anderson B Cell Lymphoma Moon Shot Project and philanthropy funds from The Gary Rogers Foundation and the Kinder Foundation. The reagent BGB-3111 was provided by BeiGene. Cell line authentication was

performed by the MD Anderson Cancer Center Characterized Cell Line Core Facility, funded by grant NCI # CA016672.

Funding Sources

This study was supported by the NIH-funded Cancer Center Support Grant (CCSG) P30 CA016672 to MD Anderson Cancer Center and the R21 CA202104 (Michael Wang, PI).

References

1. Cheah CY, Seymour JF, Wang ML. Mantle Cell Lymphoma. Journal of Clinical Oncology 2016;34(11):1256–69 doi doi:10.1200/JCO.2015.63.5904. [PubMed: 26755518]
2. Martin P, Maddocks K, Leonard JP, Ruan J, Goy A, Wagner-Johnston N, et al. Postibrutinib outcomes in patients with mantle cell lymphoma. Blood 2016;127(12):1559–63 doi 10.1182/blood-2015-10-673145. [PubMed: 26764355]
3. Cheah CY, Chihara D, Romaguera JE, Fowler NH, Seymour JF, Hagemeister FB, et al. Patients with mantle cell lymphoma failing ibrutinib are unlikely to respond to salvage chemotherapy and have poor outcomes. Annals of Oncology 2015;26(6):1175–9 doi 10.1093/annonc/mdv111. [PubMed: 25712454]
4. Bea S, Valdes-Mas R, Navarro A, Salaverria I, Martin-Garcia D, Jares P. Landscape of somatic mutations and clonal evolution in mantle cell lymphoma. Proc Natl Acad Sci USA 2013;110:18250–5. [PubMed: 24145436]
5. Kuppers R Mechanisms of B-cell lymphoma pathogenesis. Nat Rev Cancer 2005;5:251–62. [PubMed: 15803153]
6. Davis RE, Ngo VN, Lenz G, Tolar P, Young RM, Romesser PB. Chronic active B-cell-receptor signalling in diffuse large B-cell lymphoma. Nature 2010;463:88–92. [PubMed: 20054396]
7. Rahal R, Frick M, Romero R, Korn JM, Kridel R, Chan FC. Pharmacological and genomic profiling identifies NF-kappaB-targeted treatment strategies for mantle cell lymphoma. Nat Med 2014;20:87–92. [PubMed: 24362935]
8. Wu J, Liu C, Tsui ST, Liu D. Second-generation inhibitors of Bruton tyrosine kinase. Journal of Hematology & Oncology 2016;9:80 doi 10.1186/s13045-016-0313-y. [PubMed: 27590878]
9. Li Y, Bouchlaka MN, Wolff J, Grindle KM, Lu L, Qian S, et al. FBXO10 deficiency and BTK activation upregulate BCL2 expression in mantle cell lymphoma. Oncogene 2016;35(48):6223–34 doi 10.1038/onc.2016.155. [PubMed: 27157620]
10. Shinners NP, Carlesso G, Castro I, Hoek KL, Corn RA, Woodland RT. Bruton's tyrosine kinase mediates NF-kappa B activation and B cell survival by B cell-activating factor receptor of the TNF-R family. J Immunol 2007;179:3872–80. [PubMed: 17785824]
11. Tam C, Grigg AP, Opat S, Ku M, Gilbertson M, Anderson MA, et al. The BTK Inhibitor, Bgb-3111, Is Safe, Tolerable, and Highly Active in Patients with Relapsed/ Refractory B-Cell Malignancies: Initial Report of a Phase 1 First-in-Human Trial. Blood 2015;126(23):832-.
12. Rajasekaran N, Sadaram M, Hebb J, Sagiv-Barfi I, Ambulkar S, Rajapaksa A, et al. Three BTK-Specific Inhibitors, in Contrast to Ibrutinib, Do Not Antagonize Rituximab-Dependent NK-Cell Mediated Cytotoxicity. Blood 2014;124(21):3118-. [PubMed: 25232062]
13. Zhang SQ, Smith SM, Zhang SY, Lynn Wang Y. Mechanisms of ibrutinib resistance in chronic lymphocytic leukaemia and non-Hodgkin lymphoma. British Journal of Haematology 2015;170(4):445–56 doi 10.1111/bjh.13427. [PubMed: 25858358]
14. World Health Organization. Zanubrutinib. WHO Drug Information. 2018;32(1):180.
15. Hassenruck F, Knodgen E, Gockeritz E, Midda SH, Vondey V, Neumann L, et al. Sensitive Detection of the Natural Killer Cell-Mediated Cytotoxicity of Anti-CD20 Antibodies and Its Impairment by B-Cell Receptor Pathway Inhibitors. Biomed Res Int 2018;2018:1023490 doi 10.1155/2018/1023490. [PubMed: 29750146]
16. Mali P, Yang L, Esvelt KM, Aach J, Guell M, DiCarlo JE, et al. RNA-Guided Human Genome Engineering via Cas9. Science 2013;339(6121):823–6 doi 10.1126/science.1232033. [PubMed: 23287722]

17. Sanjana NE, Shalem O, Zhang F. Improved vectors and genome-wide libraries for CRISPR screening. Nat Meth 2014;11(8):783–4 doi 10.1038/nmeth.3047.

18. Wang M, Zhang L, Han X, Yang J, Qian J, Hong S, et al. A Severe Combined Immunodeficient–hu *In vivo* Mouse Model of Human Primary Mantle Cell Lymphoma. Clinical Cancer Research 2008;14(7):2154–60 doi 10.1158/1078-0432.ccr-07-4409. [PubMed: 18381957]

19. Rudelius M, Pittaluga S, Nishizuka S, Pham TH-T, Fend F, Jaffe ES, et al. Constitutive activation of Akt contributes to the pathogenesis and survival of mantle cell lymphoma. Blood 2006;108(5): 1668–76 doi 10.1182/blood-2006-04-015586. [PubMed: 16645163]

20. Yang Q, Chen LS, Ha MJ, Do K-A, Neelapu SS, Gandhi V. Idelalisib Impacts Cell Growth through Inhibiting Translation-Regulatory Mechanisms in Mantle Cell Lymphoma. Clinical Cancer Research 2017;23(1):181–92 doi 10.1158/1078-0432.ccr-15-3135. [PubMed: 27342398]

21. Fingar DC, Richardson CJ, Tee AR, Cheatham L, Tsou C, Blenis J. mTOR Controls Cell Cycle Progression through Its Cell Growth Effectors S6K1 and 4E-BP1/Eukaryotic Translation Initiation Factor 4E. Molecular and Cellular Biology 2004;24(1):200–16 doi 10.1128/MCB. 24.1.200-216.2004. [PubMed: 14673156]

22. Portell CA, Axelrod M, Brett LK, Gordon VL, Capaldo B, Xing JC, et al. Synergistic Cytotoxicity of Ibrutinib and the BCL2 Antagonist, ABT-199(GDC-0199) in Mantle Cell Lymphoma (MCL) and Chronic Lymphocytic Leukemia (CLL): Molecular Analysis Reveals Mechanisms of Target Interactions. Blood 2014;124(21):509-.

23. Zhao X, Bodo J, Sun D, Durkin L, Lin J, Smith MR. Combination of ibrutinib with ABT-199: synergistic effects on proliferation inhibition and apoptosis in mantle cell lymphoma cells through perturbation of BTK, AKT and BCL2 pathways. Br J Haematol 2015;168:765–8. [PubMed: 25284608]

24. Tam CS, Anderson MA, Pott C, Agarwal R, Handunnetti S, Hicks RJ, et al. Ibrutinib plus Venetoclax for the Treatment of Mantle-Cell Lymphoma. N Engl J Med 2018;378(13):1211–23 doi 10.1056/NEJMoa1715519. [PubMed: 29590547]

25. Xu B-e, Lee B-H, Min X, Lenertz L, Heise CJ, Stippec S, et al. WNK1: analysis of protein kinase structure, downstream targets, and potential roles in hypertension. Cell Res 2005;15(1):6–10. [PubMed: 15686619]

26. Shekarabi M, Zhang J, Khanna AR, Ellison DH, Delpire E, Kahle KT. WNK Kinase Signaling in Ion Homeostasis and Human Disease. Cell Metabolism;25(2):285–99 doi 10.1016/j.cmet. 2017.01.007.

27. McCormick JA, Ellison DH. The WNKs: Atypical Protein Kinases With Pleiotropic Actions. Physiological Reviews 2011;91(1):177–219 doi 10.1152/physrev.00017.2010. [PubMed: 21248166]

28. Friedel P, Kahle KT, Zhang J, Hertz N, Pisella LI, Buhler E, et al. WNK1-regulated inhibitory phosphorylation of the KCC2 cotransporter maintains the depolarizing action of GABA in immature neurons. Science Signaling 2015;8(383):ra65-ra doi 10.1126/scisignal.aaa0354. [PubMed: 26126716]

29. Kochl R, Thelen F, Vanes L, Brazao TF, Fountain K, Xie J, et al. WNK1 kinase balances T cell adhesion versus migration in vivo. Nat Immunol 2016;17(9):1075–83 doi 10.1038/ni.3495. [PubMed: 27400149]

30. Jiang ZY, Zhou QL, Holik J, Patel S, Leszyk J, Coleman K, et al. Identification of WNK1 as a Substrate of Akt/Protein Kinase B and a Negative Regulator of Insulin-stimulated Mitogenesis in 3T3-L1 Cells. Journal of Biological Chemistry 2005;280(22):21622–8 doi 10.1074/ jbc.M414464200. [PubMed: 15799971]

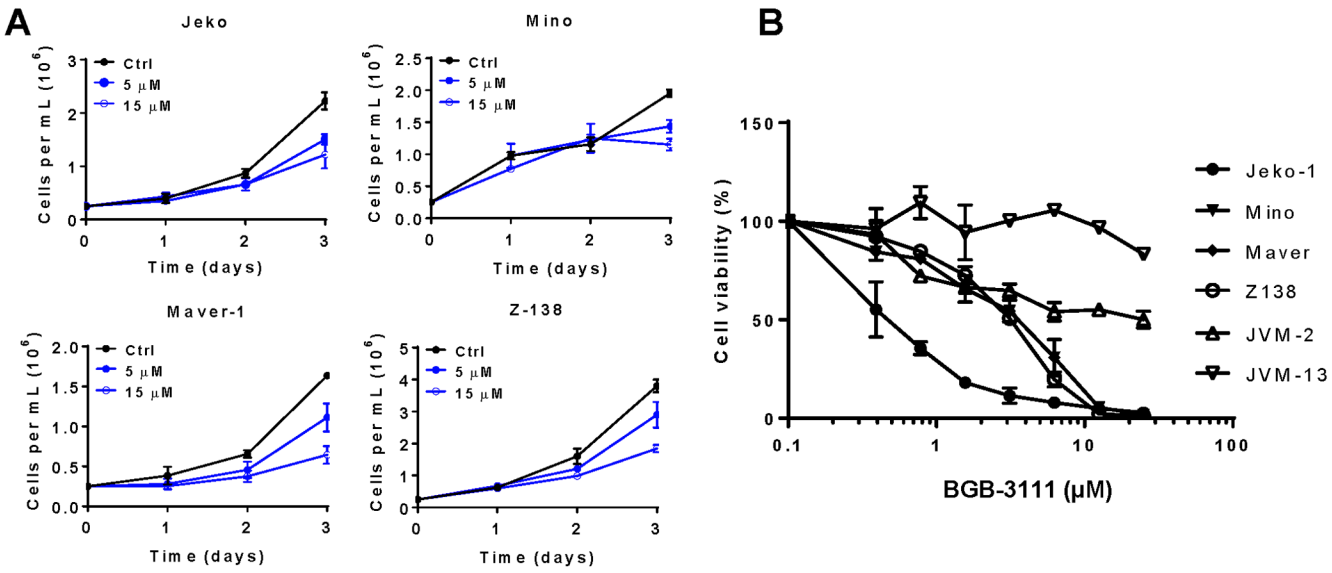

Figure 1. BGB-3111 inhibits BTK phosphorylation and MCL cell proliferation.

A, BGB-3111 inhibits cell proliferation in a dose-dependent manner. Cells were cultured in 5 or 15 μM BGB-3111. Cell numbers were calculated via the trypan blue exclusion test. B, Cell viability of MCL cell lines following 72 hr treatment with BGB-3111 (left). Drug concentrations are as follows: 0.03, 0.1, 0.3, 1, 3, 10, and 30 μM. Luminescence was quantified by Cell TiterGlo Reagent and presented as the mean ± SD of triplicate values.

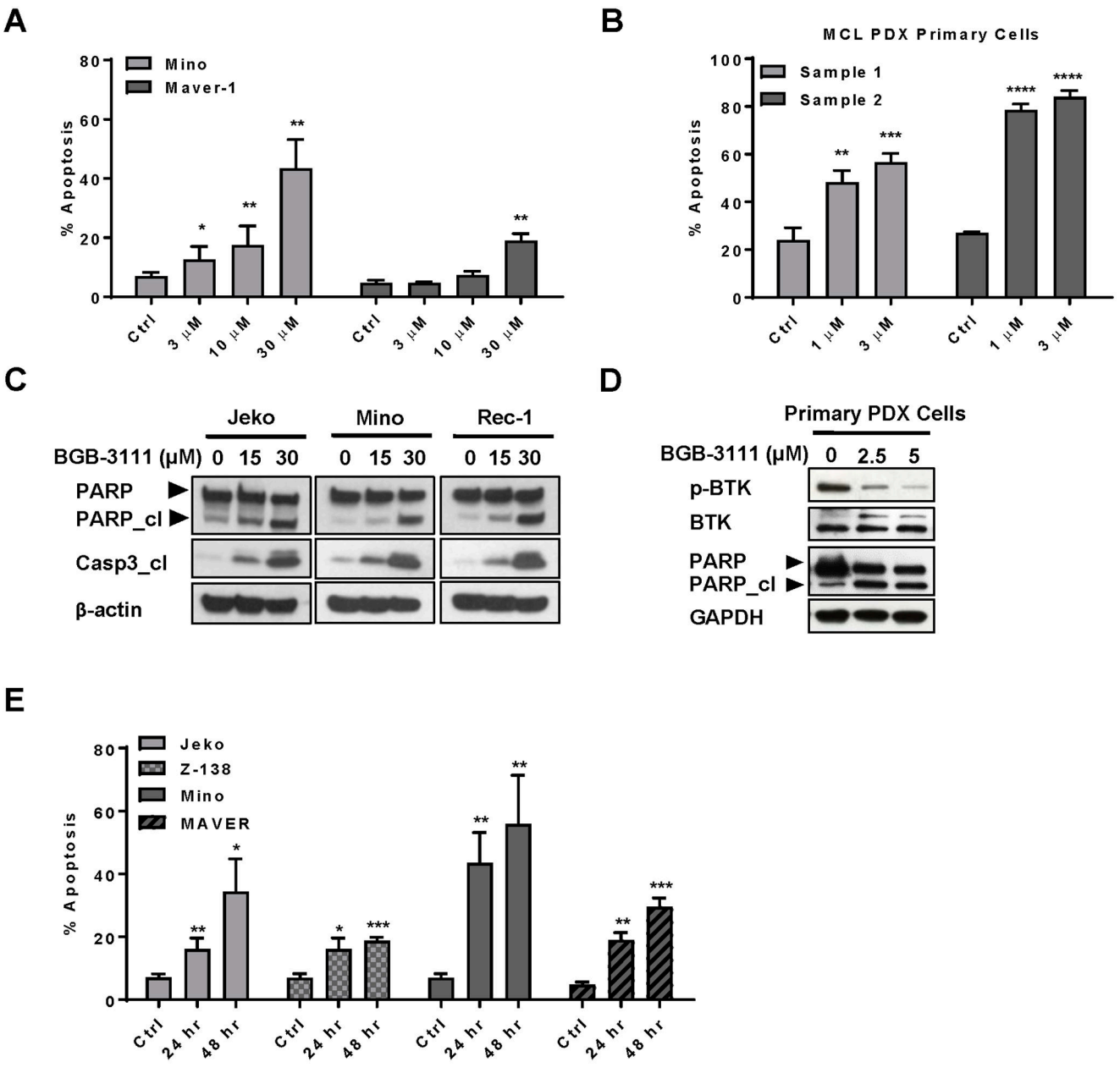

Figure 2. BGB-3111 induces apoptosis in immortalized and primary MCL cells.

A, BGB-3111 induces concentration-dependent apoptosis, as measured by Annexin V/PI staining and flow cytometry. B, Apoptotic induction in primary MCL cells isolated from PDX tumor tissue following BGB-3111 treatment. MCL cells were incubated with the indicated concentrations for 16 hrafter establishing short term primary cell cultures. C-D, Immunoblotting of cleaved PARP and caspase-3 in MCL cell lines (left) and primary cells (right) isolated from MCL PDX tumor tissue. E, BGB-3111-induced apoptosis over 24 to 48 hours after treatment with 30 μM BGB-3111. Apoptotic cell population was determined as in (A). All data are presented as mean % apoptosis ± SD of three or more independent experiment measurements. *P < .05; **P < .01, ***P < .001, ****P < 0.0001.

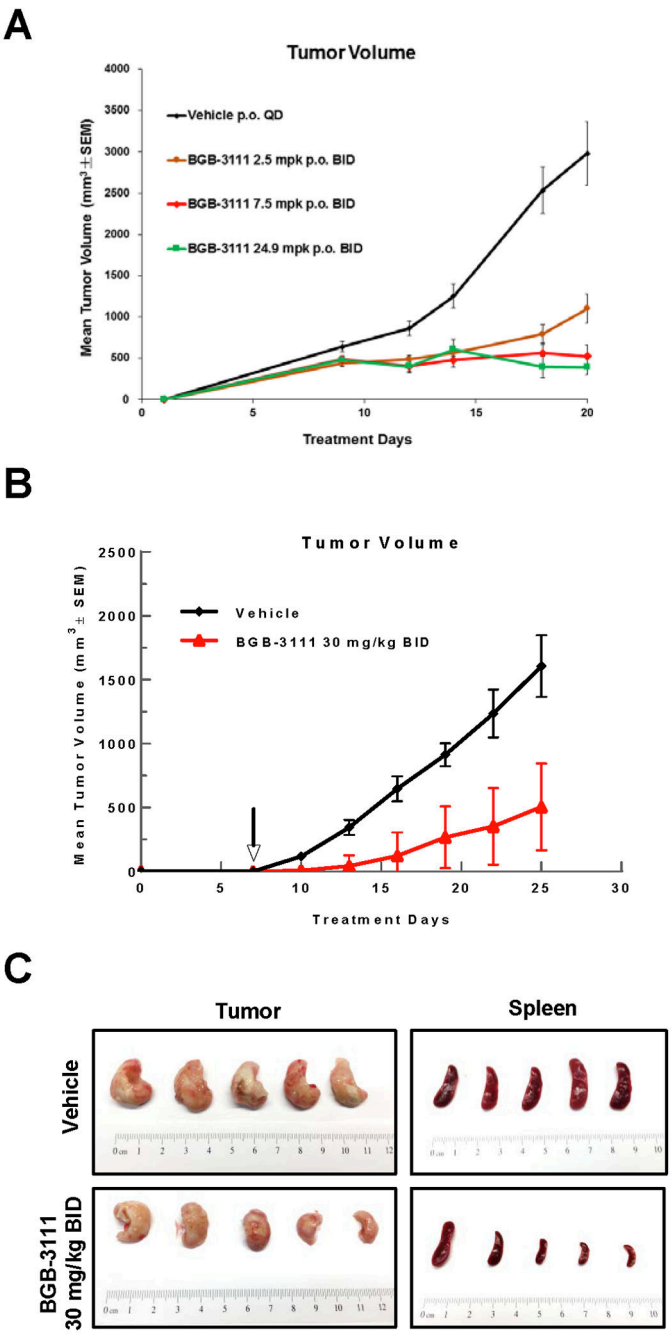

Figure 3. Tumor growth inhibition by single agent BGB-3111 treatment in MCL subcutaneous (s.c.) and PDX models.

A, Efficacy of BGB-3111 in Rec-1 s.c. xenograft model (n=10). B, Efficacy of single agent BGB-3111 in MCL PDX model. Vehicle control (n=5); 30 mg/kg BGB-3111 oral gavage BID (n=5). C, Images of resected tumor and spleen from each cohort, as indicated.

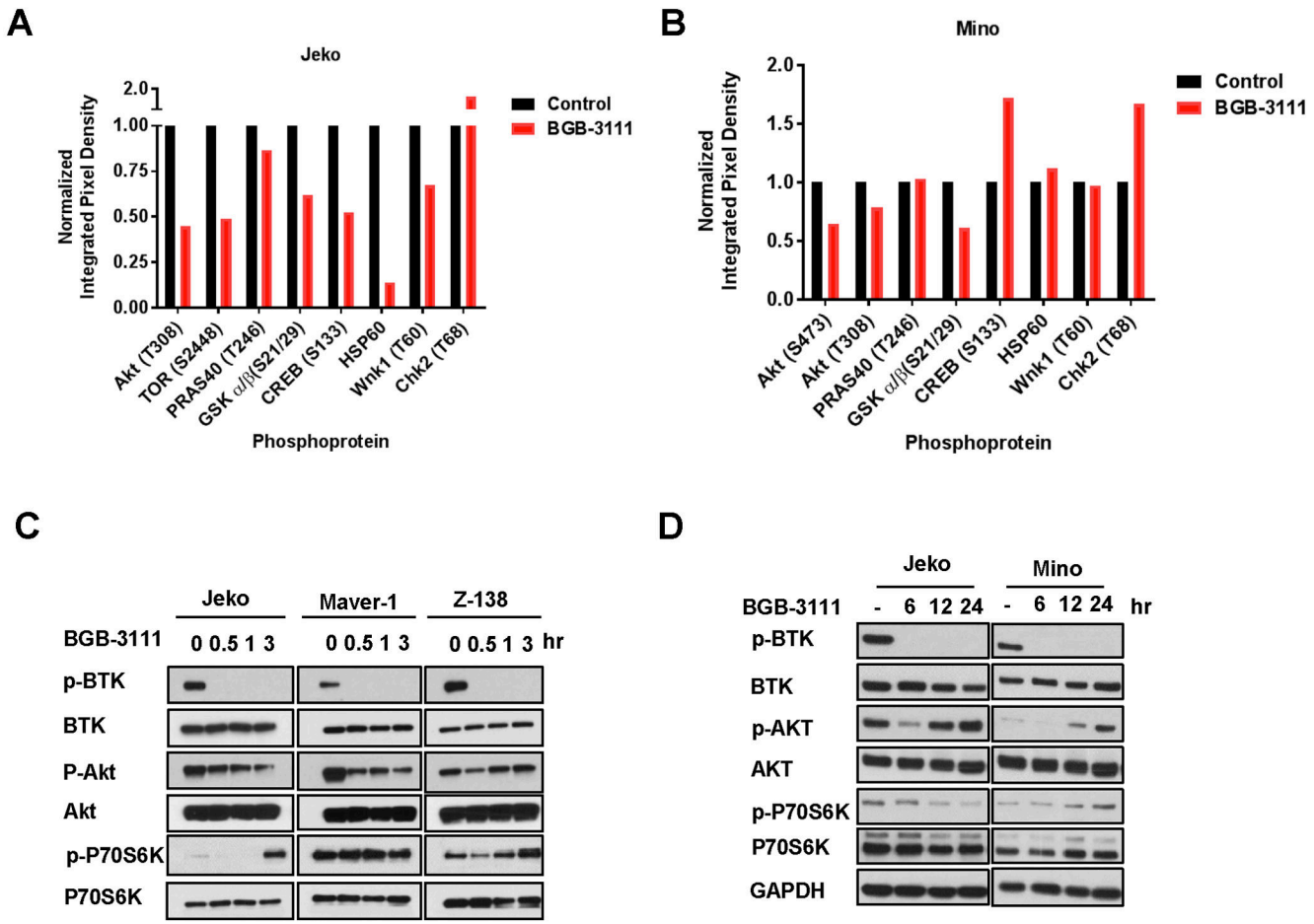

Figure 4. Effects of BGB-3111 on signal transduction in MCLs.

A-B, Phosphokinase profiling array of Jeko (left) and Mino (right) cells treated with 5 μM BGB-3111 for 1 hr. Integrated pixel density values were normalized to untreated control. C, Immunoblotting of major growth/survival signaling kinases in MCL cell lines in response to 5 μM BGB-3111 at 0, 30 min, 1 hr, or 3 hr. C, Immunoblotting of p-Akt, p-PLCγ2, and p-P70S6K in Jeko cells treated with 15 μM BGB-3111 and collected at the indicated time points. D, Immunoblotting of p-Akt, p-PLCγ2, and p-P70S6K in Jeko and Mino cells treated with 15 μM BGB-3111 and collected at the indicated time points.

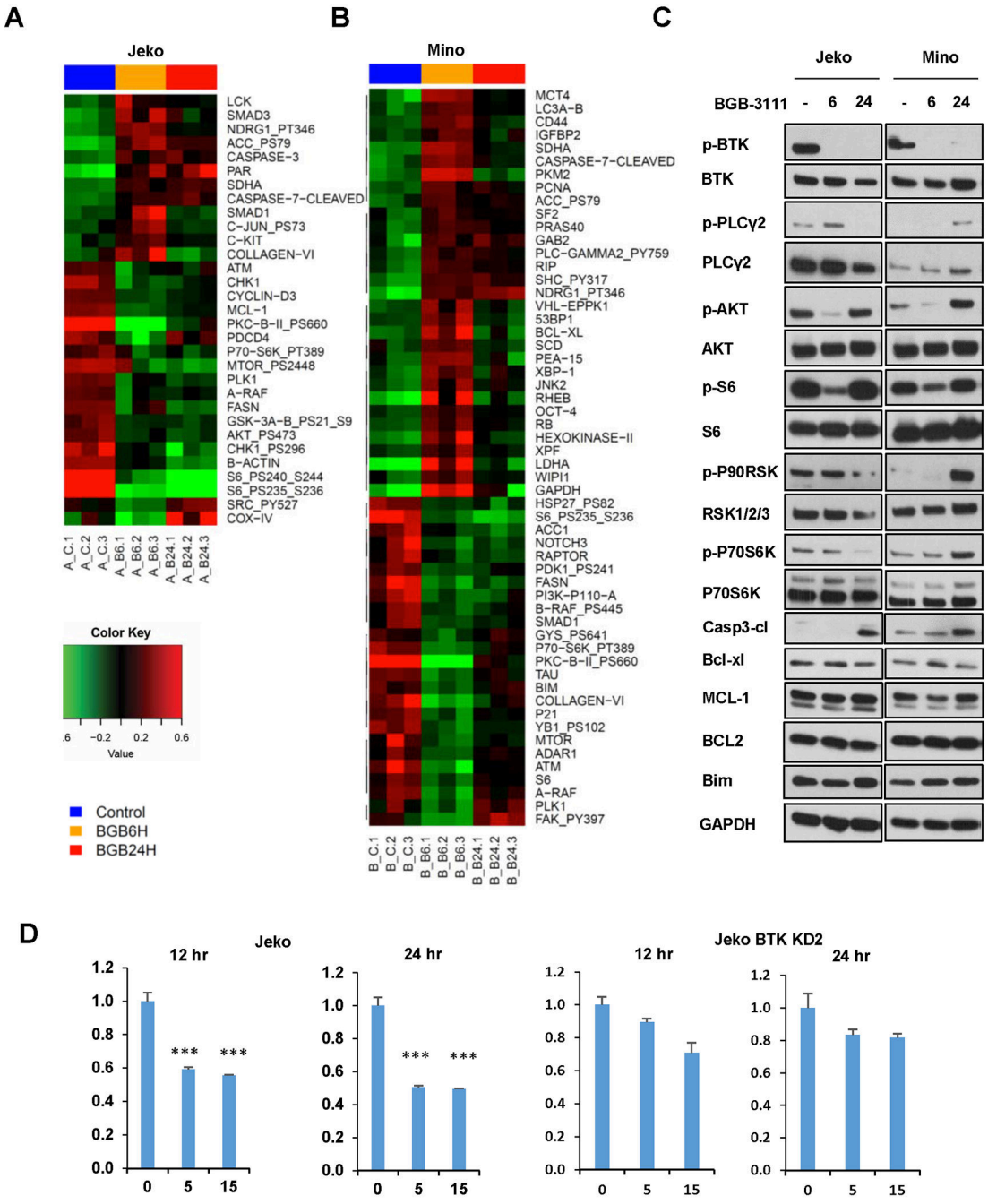

Figure 5. RPPA profiling of BGB-3111 treatment in two MCL cell lines in triplicate following 0, 6, and 24 hr.

Individual heat maps of differential protein expression in Jeko cells A, and Mino cells B, treated with BGB-3111 as generated by one-way ANOVA analysis. Each data point consists of three technical replicates. C, Immunoblotting of lysates from Jeko and Mino cells treated with 15 μM BGB-3111 at the indicated time points. D, NF-κB transcription activation reporter assay in Jeko cells and BTK-KD2 cells treated with 15 μM of BGB-3111 and harvested at 12 and 24 hr for the luciferase assay. Error bars depict standard deviation derived from three biological repeats. ***, $p < 0.0001$.

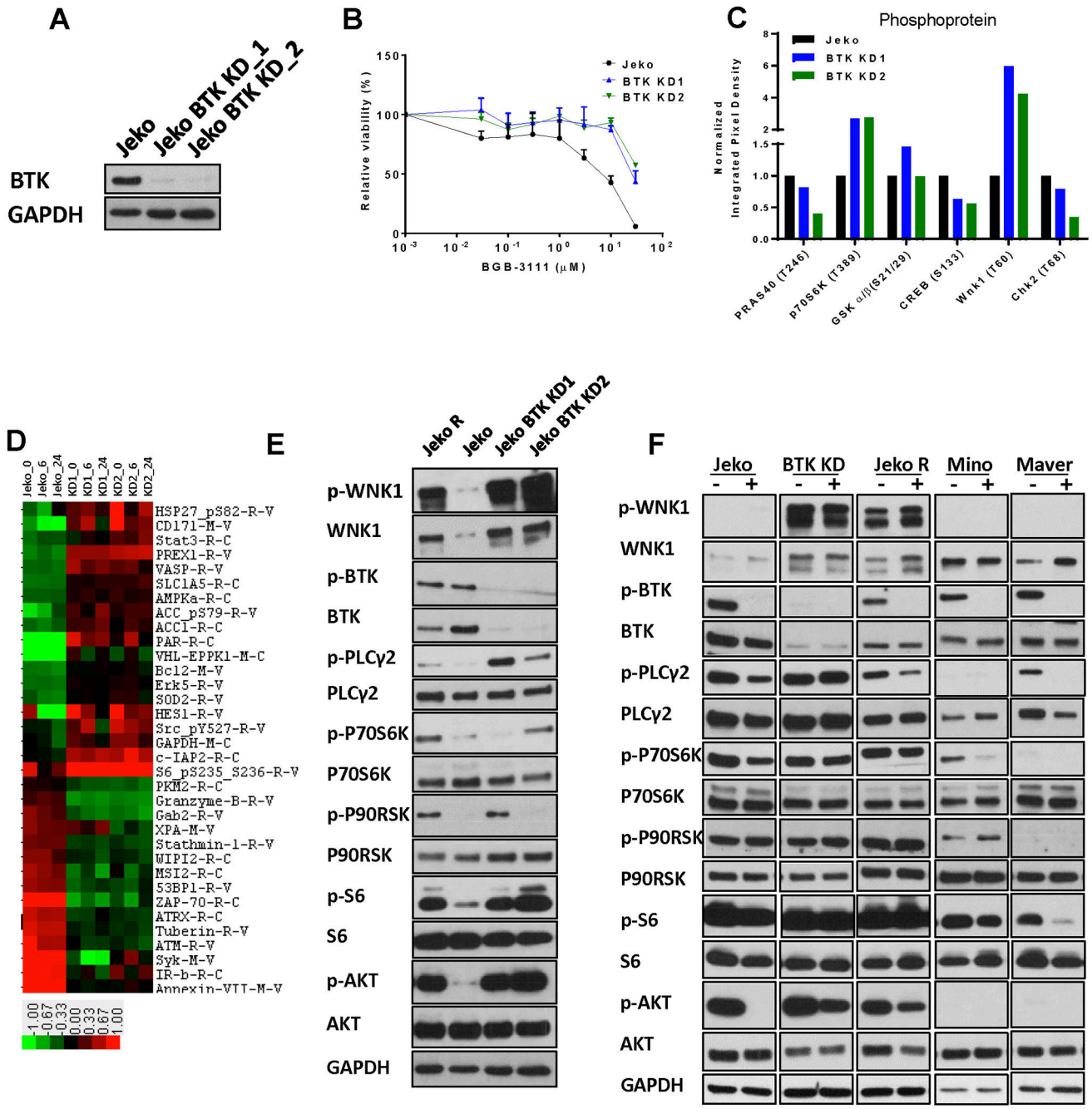

Figure 6. BTK knockdown model confers resistance to BGB-3111.

A, Immunoblotting of BTK in parental Jeko cells and two BTK knockdown Jeko BTK-KD1 and BTK-KD2 clones. B, Drug sensitivity of Jeko, BTK-KD1, and BTK-KD2 to BGB-3111. Cell survival was measured following 72-hour treatment with serial concentrations of BGB-3111. Note: the Jeko mock treatment control is identical to that of Fig. 1C because both experiments were carried out in the same set of triplicate 96-wells. C, Steady-state phosphokinase activation in Jeko, BTK-KD1, and BTK-KD2 as determined by quantitative phosphokinase array. D, RPPA profiling of BGB-3111 treatment in Jeko, BTK-KD1, and

BTK-KD2 in triplicate following plating for 0, 6, and 24 hr. Heat maps of differential protein expression in these cells were shown. Each data point consists of three technical replicates. E, Validation of differential protein expression in Jeko, Jeko R, and BTK knockdown cells by immunoblotting. F, Immunoblotting of differential protein expression in Jeko, Jeko R, BTK knockdown mutant, Mino and Maver cell lines exposed to BGB-3111 for three hours.